Pseudo Body Surface Potential Mapping on Heart using 3D Wavelet Transform

Amr Sharawy
Faculty of Engineering, Cairo University, Egypt

Sherief Samy
Faculty of Engineering, Cairo University, Egypt

Mohamed Aouf
Higher Technological Institute, Egypt

ABSTRACT
Body surface potential mapping (BSPM) is used to detect real diagnostic information about the myocardium state more than the standard 12-lead electrocardiogram (ECG). The present research introduces a practical solution for recording body surface potential maps using the standard 12-lead ECG with different positions. It is called pseudo BSPM where all channels were not read out simultaneously. It is based on the assumption that heart beat body surface potential mapping (BSPM) is used to detect real diagnostic information about the myocardium state more than standard 12-lead electrocardiography (ECG). Pseudo BSPM pattern is not changed considerably during the whole measurement session. Body surface potential mapping was applied to normal and abnormal persons suffering from coronary heart diseases (CHD). We detect QRS complexes using filter banks and consequently build up a cardiac map using 3D wavelet transform. Our results for the cardiac map demonstrate the changes that occur for the cardiac electrical activity which represents the patient case in color degradation patterns.

General Terms
Pattern Recognition. Signal Processing, Waveform Analysis

Life and Medical Science, Wavelets and Fractals.

Keywords
ECG; Body Surface Potential Mapping; Cardiac mapping; Filter banks; Wavelet Transform

1. INTRODUCTION
Body surface potential mapping is an important method to enhance the power of diagnostic of traditional 12-lead ECG [1] [2] [3]. In the present research we use the traditional 12-lead ECG for mapping the heart biopotential by changing the positions of chest leads. The heart is an electrically closed conducting shell, assuming that of negligible thickness that contains dipoles. From the huge number of heart diseases, there are two main classes; the first class is the coronary heart diseases (CHD) and the second class is arrhythmia. Body surface potential mapping techniques helps to diagnose both classes [4]. A crucial part of any ECG processing algorithm is QRS beat detection. Reference [5] presents original work for QRS detection. Figure 1 shows the proposed processing stages for body surface potential mapping based on the 3D wavelet transform.

For ECG beat detection algorithms we use pre-processing filters to maximize the signal to noise ratio (SNR). To obtain the QRS complex of the ECG waveform we apply stages of nonlinear processing and moving window integration. For QRS detection we deal with signal peaks and noise peaks.

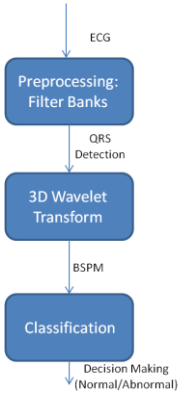

Fig. 1: Processing chain performed on the ECG.

Using optimal thresholding we can differentiate between QRS complexes and noise peaks.

In some cases the ECG signal may pass without QRS detection; thus a "search-back" strategy technique is used to check the QRS again. Sometimes search-back strategy is not helpful for the immediate indication of the occurrence of QRS.

Filter banks play an important role in beat detection of ECG. The basic design of filter banks is shown in Figure 2. Filter banks are composed of analysis filters and synthesis filters.

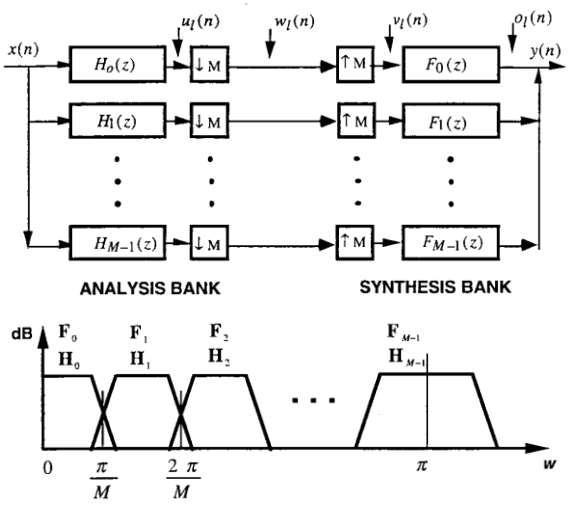

Fig. 2: Filter banks design and theory

The analysis filters are used to decompose the bandwidth of the input ECG signal into sub-band signals with uniform frequency bands, down-sampling the input signal as a multirate digital signal. These sub-bands can be then reconstructed using the synthesis filters. Before introducing the synthesis filters we use up-sampling. References [6-11] cover how to apply filter banks to increase signal to noise ratio.

Wavelet transform is a relative recent development in applied mathematics. It is a mathematical tool with a great variety of possible applications. It has already led to exciting applications in biomedical signal analysis (ECG, EEG, and EMG) and numerical analysis; many other applications are being studied [13]. The first recorded mention of the term "wavelet" was in 1909 in a thesis by Alfred Haar [14][15]. However, the concept of wavelets in its present theoretical form was first proposed by Jean Morlet and the team at the Marseille Theoretical Physics Center working under Alex Grossmann in France. Y. Mayer and his colleagues have developed the methods for wavelet analysis. The main algorithm dates back to the work of Stephanie Mallet in 1988. Since then, research on wavelets has been international [16].

Daubechies is one of the brightest stars in the world of wavelet research invented what are called compactly supported orthonormal wavelets, thus making discrete wavelet analysis practicable.

Daubechies family includes the Haar wavelet, written as DB1, the simplest wavelet imaginable and certainly the earliest [17]. The authors in [18] investigated the application of wavelet denoising in noise reduction of multichannel high resolution ECG signals implemented in the MatLab environment. The procedure of noise reduction in signal $x_i(t)$ in the i-th channel is based on decreasing the noise content in high frequency components (details) of signal. They have tested 19 wavelet functions: Daubechies proposed functions [19] (db2, db3, db4, db5, db6, db7, db8), and their modifications, so-called Symlets wavelets (sym2, sym3, sym4, sym5, sym6, sym7, sym8), as well as bi-orthogonal wavelets (bior3.3, bio4.4, bio6.8). A useful discussion of the difference and usage of the db functions can be found in [23]. Interesting results of noise reduction support also the application of wavelet sym8 for 5th level of decomposition. This function allows for good approximation of parts of ECG with lower frequency components P wave and T wave. However, it is done at expense of higher frequency components of ECG signal and affects morphology of the QRS complex. In Reference [20], wavelet neural network (WNN) is studied for ECG signal modeling and noise reduction. WNN combines the multi-resolution nature of wavelets and the adaptive learning ability of artificial neural networks.

The concept of Wavelet Neural Network (WNN) was inspired by both the technologies of wavelet decomposition and neural networks. In standard neural networks, the input-output mapping is approximated by the superposition of sigmoid functions, while in WNN this relationship is approximated by the superposition of a series of wavelet functions. In [21] the authors proposed a new approach to filter the ECG signal from noise using Wavelet Transform. Using Mayer wavelet implemented on MATLAB, the recorded ECG had a sampling frequency 400 Hz, spectral band of frequency 0.5-70 Hz and a standard deviation of 0.9. The basic aim of the proposed method was to perform the DWT of the signal. Then the transform passed through a threshold to remove the coefficients below a certain value. Finally, the Inverse DWT (IDWT) was used to reconstruct the denoised signal. A similar method proposed in [21], however, has used different ECG signals from the MIT/BIH arrhythmia database with added 10dB, 5dB & 0dB Power Line Interference (PLI) noise which is common in ECG signals. The results were evaluated using MATLAB.

Thus, the wavelet transform was very successful to analyze the ECG. We propose to utilize the wavelet transform to replace the conventional Fourier analysis for the body surface potential mapping.

2. MATERIAL AND METHODS

The material of this paper is composed of the subjects and equipment used.

Our subjects are 10 normal and 10 abnormal adult male cases, aged from 21 to 28, having a weight range from 60 to 100 kg and a height range from 1.2 to 1.7 meters. The equipment used is an ECG, model Heart Mirror IKO, having one channel with 12 lead selectors interfaced with a computer special designed for this experiment.

The ECG circuit's amplifier frequency response is 0.05 Hz-150 Hz. The maximum input noise is 25 μV-pp. The minimum CMRR is 100 dB. The DC tolerance is +320 mV DC. The minimum input impedance is 20MΩ. The input signal range is ± 5 mV. The sampling frequency is 200 Hz (assuming the maximum frequency of the signal f_{max} = 100 Hz). The trace sensitivity is 0.25cm/mV. There is also a 50-Hz line noise rejection filter and a 35-Hz muscle noise rejection filter in the circuit. The recording time in automatic mode is 3 sec at a 25 mm/sec and 1.5 seconds at 50mm/sec speed. The operating temperature range is +10°C to +40°C. The power supply is a built-in power supply with an input voltage of 220 V and a nominal output power of 5.5 VA.

Our experiment was conducted at Cairo Medical Center Hospital. We applied our practical cases as shown in Fig. 3, applying different lead positions on the chest. The ordinary position (P0), the upper positions (P1) and (P2), and the lower positions (P3) and (P4) are shown in Fig. 3.

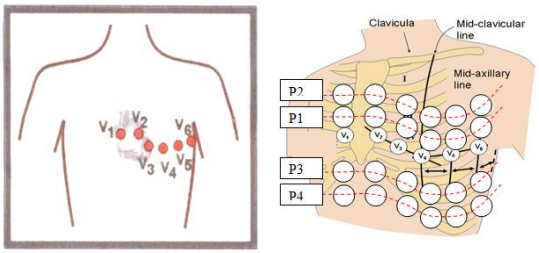

(a) (b)

Fig 3: Chest leads Positions (a) Standard (b) New research positions (P1-P2-P3-P4)

Our methodology deals with data acquisition (in the form of data collection at different positions over patient chest). In the processing stage we first detect the QRS as shown in Fig. 4. Then we plot the whole signal and average cardiac cycle in the time domain. Finally we draw the maps and contours for the whole signal and average cardiac cycle.

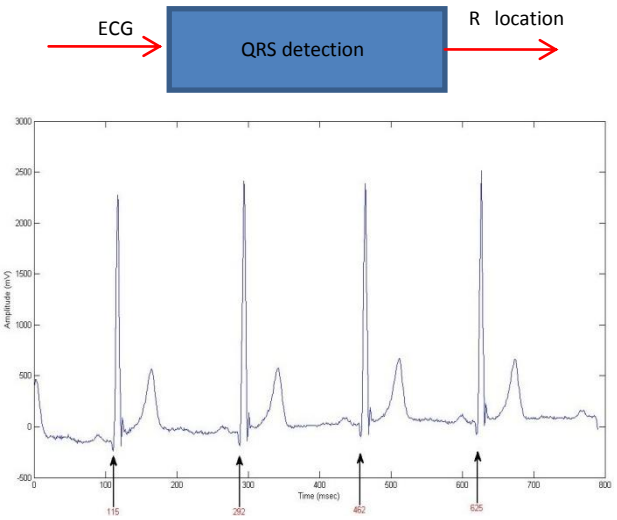

Fig. 4: QRS detection

For beat detection (QRS), filter banks (FB) are used with finite impulse response filters (FIR) without any aliasing error and without any magnitude or phase distortion. The selected filter bandwidth is 5.6 Hz. Each of the filters used are linear phase. Our filter banks have a down sampling stage. For the down sampling process; filters are adjusted to operate every 32 samples. Down sampling helps us to decrease computational effort and cost. The goal of the detection algorithm is to get real (QRS) signals without noise. For real detection of QRS we are maximizing the number of true positives (TPS) while minimizing other assumptions.

Wavelets provide a tool for time and frequency localization. If one analyzes a function *f(t)* by means of wavelets then there will definitely be some kind of localization. Transient features (short-time details) of *f(t)*, like jump discontinuities or peaks can easily be localized in the wavelet coefficients of small scales. Long time trends of *f(t)* are stored in deeper layers of the coefficient hierarchy and are automatically represented in larger scales. As a consequence they are less precisely localized on the time axis.

The wavelet analysis of a signal gives two sub-bands: the approximation and the details. The approximation is generated using an additional function called the scaling function $\phi(t)$. It shows information about slow changes in the signal. This is due to the fact that it contains only the low frequency components of the signal. The details are generated by the wavelet function $\psi(t)$; it shows the high frequencies carried by the signal and hence the rapid changes in the signal; therefore it can be easily used to discover the discontinuity points in the signal [16].

A set of wavelet functions $\{\Psi_{a,b}(t)\}$ can be generated by scaling and translating the mother wavelet $\Psi(t)$ by quantities a, b, respectively as:

$$c(b,a) = \int_{-\infty}^{\infty} f(t)\psi_{(b,a)}(t)dt \qquad (1)$$

Where a > 0 and b are real numbers.

The inverse wavelet transform using the wavelets $\{\Psi_{a,b}(t)\}$ can be written as follows:

$$f(t) = \int_a \int_b \frac{1}{a^2} c(b,a)\psi_{(b,a)}(t)dbda \qquad (2)$$

The wavelet transform is the representation of the signal *f(t)* in terms of the wavelet coefficients *c(a,b)*. The wavelet analysis can be extended from 1D signal into images. The sub-bands are represented by three 2D wavelets and a 2D scaling function as [2]:

$$\Psi^{[1]}i, j(x,y) = \Phi(x-i)\Psi(y-j) \qquad (3)$$
$$\Psi^{[2]}i, j(x,y) = \Psi(x-i)\Phi(y-j) \qquad (4)$$
$$\Psi^{[3]}i, j(x,y) = \Psi(x-i)\Psi(y-j) \qquad (5)$$
$$\Phi_{i,j}(x,y) = \Phi(x-i)\Phi(y-j) \qquad (6)$$

A one level of analysis results in one approximation and three details. The approximation A represents the image at a coarser resolution; it results from averaging in both directions of the image, x and y directions. The horizontal details H are obtained by averaging in x-direction and differencing in the y-direction. The vertical details V are obtained by averaging in y-direction and differencing in the x-direction. The diagonal detail D is obtained by differencing in both directions. Horizontal edges tend to show up in H and vertical edges in V, while D contains all other details [15]. The 3D scaling function and the 3D wavelet functions can each be expressed as a product of three one-dimensional functions. The analysis is carried out along the x-dimension, the y-dimension, and the z-dimension of the volumetric data. Eight coefficients result from the one level analysis. One coefficient represents a volume approximation of the input data. The information which is missed in the approximation is distributed in the other 7 volume detail coefficients [13][22].

$$\emptyset_{j,\{k,l,m\}}(x,y,z) = 2^{3j/2}\,\emptyset(x-2^{-j}k)\,\emptyset(y-2^{-j}l)\,\emptyset(z-2^{-j}m) \qquad (7)$$
$$\psi^{1}_{j,\{k,l,m\}}(x,y,z) = 2^{3j/2}\,\psi(x-2^{-j}k)\,\emptyset(y-2^{-j}l)\,\emptyset(z-2^{-j}m) \qquad (8)$$
$$\psi^{2}_{j,\{k,l,m\}}(x,y,z) = 2^{3j/2}\,\emptyset(x-2^{-j}k)\,\psi(y-2^{-j}l)\,\emptyset(z-2^{-j}m) \qquad (9)$$
$$\psi^{3}_{j,\{k,l,m\}}(x,y,z) = 2^{3j/2}\,\Psi(x-2^{-j}k)\,\psi(y-2^{-j}l)\,\emptyset(z-2^{-j}m) \qquad (10)$$
$$\psi^{4}_{j,\{k,l,m\}}(x,y,z) = 2^{3j/2}\,\emptyset(x-2^{-j}k)\,\emptyset(y-2^{-j}l)\,\psi(z-2^{-j}m) \qquad (11)$$
$$\psi^{5}_{j,\{k,l,m\}}(x,y,z) = 2^{3j/2}\,\psi(x-2^{-j}k)\,\emptyset(y-2^{-j}l)\,\psi(z-2^{-j}m) \qquad (12)$$
$$\psi^{6}_{j,\{k,l,m\}}(x,y,z) = 2^{3j/2}\,\emptyset(x-2^{-j}k)\,\psi(y-2^{-j}l)\,\psi(z-2^{-j}m) \qquad (13)$$
$$\psi^{7}_{j,\{k,l,m\}}(x,y,z) = 2^{3j/2}\,\psi(x-2^{-j}k)\,\psi(y-2^{-j}l)\,\psi(z-2^{-j}m) \qquad (14)$$

For the conventional 3D transform the input is a cubic shape data element with three dimensions, width, height, and depth. In this case the smallest number of sample points is eight, two- sample points along each dimension.

For multiple level analyses the input data must be at least of size 2j where j is the desired analysis level [13][22].

3. RESULTS AND DISCUSSION

This section presents the results of each experiment followed by in-depth interpretation and discussion of these results, showing the reasons for unexpected outcomes. The supplied program gives the ability to load any cases saved in the hard disk. After cases have been loaded, the user can perform different kinds of analysis on the loaded data.

This section deals with the display of the measurements in the time domain, in form of 3D-maps using the wavelet transform.
Two options are given to user: the first of them to draw the whole signal, and the second one to draw the average cardiac cycle.

Simply, the user chooses the position of electrode to be plotted from (P0 to P4) and also the channel (from V1 to V6). Then the program plots the signal. Fig. 5 shows the whole ECG signal plot.

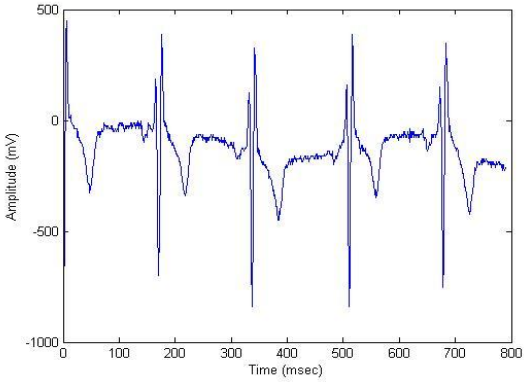

Fig. 5. Whole ECG signal plot

Using a code to detect the QRS complex, the chosen signal is divided according to the detected QRS. All the divided parts of the signal are plotted together. Fig. 6 displays the detected cardiac cycle and the average cardiac cycle.

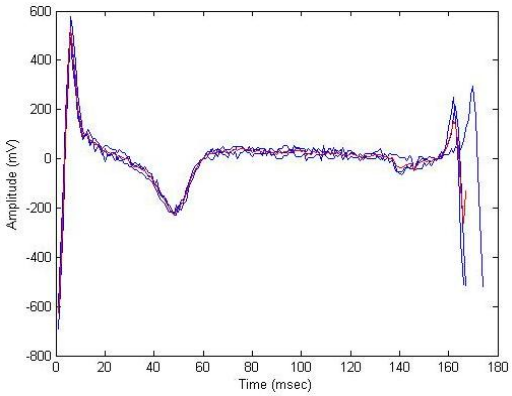

Fig. 6. Cardiac cycle and average cardiac cycle; the blue lines represent the detected cardiac cycles, while the red line represents the average cycle

Finally the user can plot all the signals at different positions from P0 to P4 and all the channels (from V1 to V6). Fig. 7 shows the various signal plots.

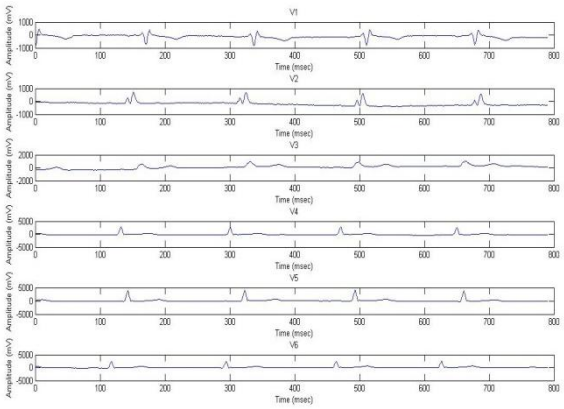

Fig 7: The plots of ECG signal at different positions

Fig. 8 displays the contours for the average cardiac cycle for a normal person. Similar contours can be drawn for abnormal persons.

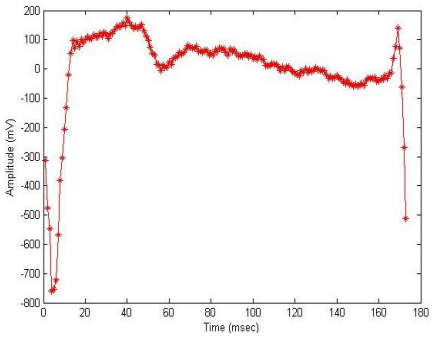

Fig. 8. The average cardiac cycle for a normal person

Fig. 9 shows us the percentage average error in the contour plot of the five positions (P0-P1-P2-P3-P4) of the chest leads.

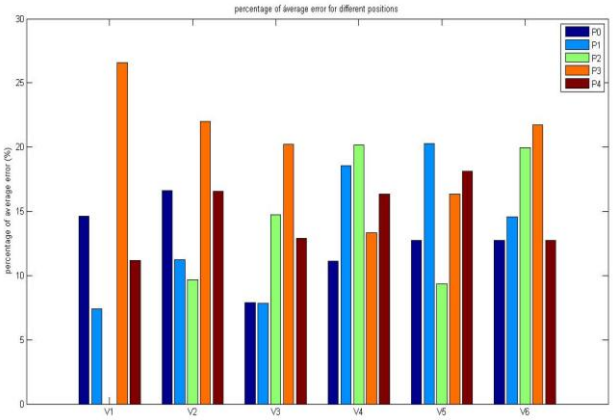

Fig 9: Percentage of average error for different positions

We applied the experiment on 10 normal persons and 10 patients suffering from coronary heart disease at ICU of the hospital. Fig. 10 shows the comparison between normal and abnormal cases using the 3D wavelet transform measurements at different times.

4. CONCLUSIONS

The output of the experiment shows significant difference between maps of normal state and coronary heart disease at different times.

At the first 10 msec.: We observe high –ve peaks at P2 with V3, P2/V5, P0/V3, P0/V5, P4/V3 and P4/V5 for normal cases. But for abnormal cases we observed +ve values appear at P0/V1, P0/V3, P4/V1 and P4/V3.

At the first 20 m sec.: We observed –ve peaks at P4/V1 and +ve values at P2/V1, P2/V3, P0/V1, P0/V3, P0/V5, P4/V3 and P4/V5 for normal case. For abnormal cases we got similar results, however with certain difference, that is we got no –ve peaks at all.

At the first 30 m sec.: Approximately all positions record highly negative peaks for normal cases. But for abnormal cases, approximately zero potential occurs at P2/V3, P2/V4.

At the first 40 m sec.: Most positions record high negative peaks for normal and abnormal cases without any change.

5. ACKNOWLEDGMENTS

Our thanks to Dr. Mohammed Abdel-Megeed Salem for his contribution on the theory of the 3D wavelet transform.

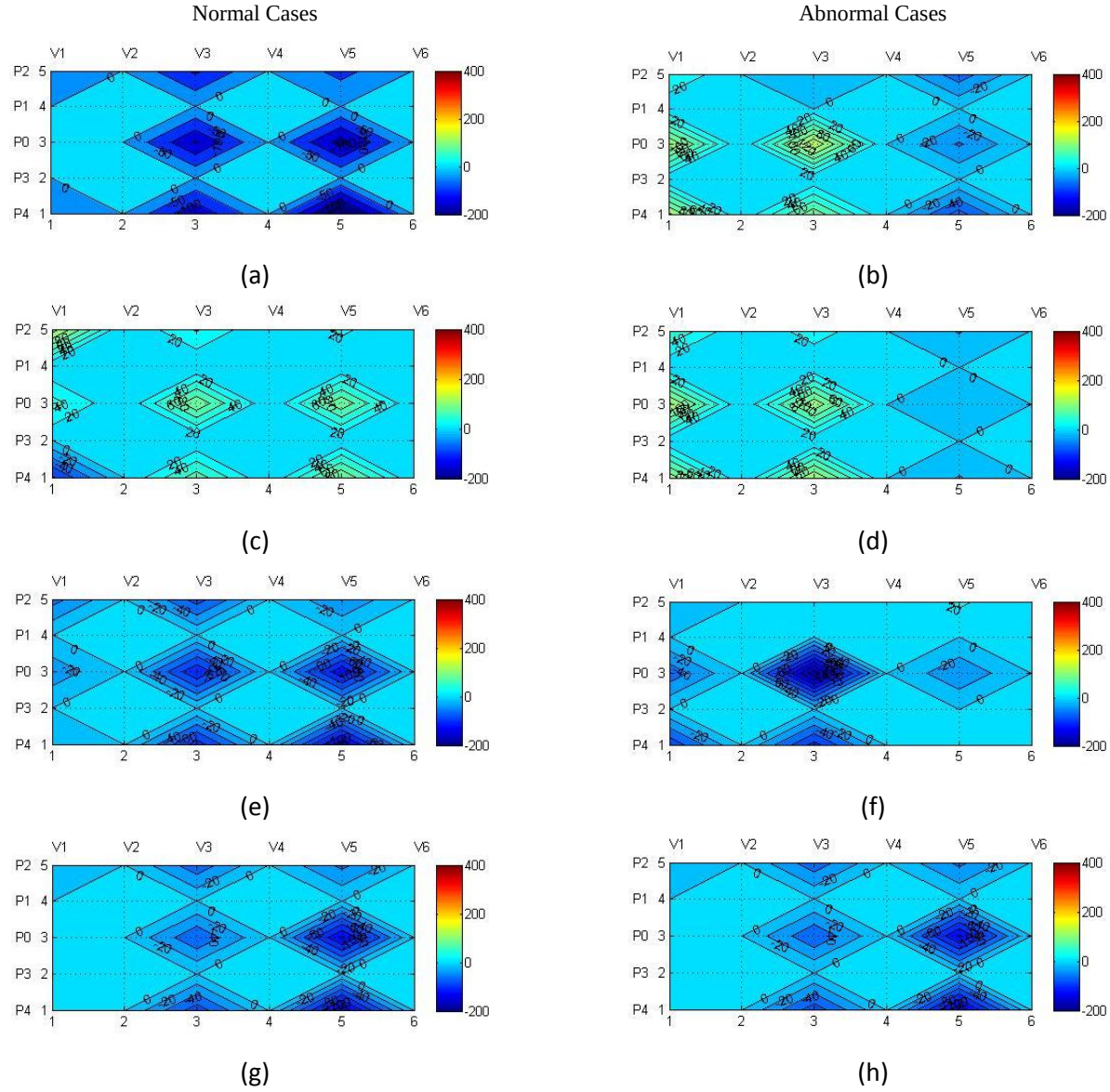

Fig 10. Comparison between BSPM for normal and abnormal patient suffering from coronary heart diseases using 3D wavelet transform. figures a, c ,e, and g represent normal cases. The others represent the abnormal cases.

6. REFERENCES

[1] N.c. FLOWERS and L. G.HORAN."BODY SURFACE POTENTIAL MAPPING", in cardiac electrophysiology: From cell to Bedside, 2nd ed ,D. P. Zipes and J . Jalife , Eds . Philadephia ,PA : WB Saunders , 1995 , pp . 1049-1067

[2] "BODY SURFACE POTENTIAL MAPPING", in cardiac electrophysiology: From cell to Bedside, 3 ed ,D. P. Zipes and J . Jalife , Eds . Philadephia ,PA : WB Saunders , 2000 , pp .737-746

[3] P . W .Macfarlane and T. D . Veitch Lawrie , Eds.,"Compressive electrocardiology – theory and practice in health and disease , "in lead systems. New York : Pergamon , 1989 , vol . 1 ch . 11 . cf..

[4] L.S. "effects of ischemia on cardiac electrophysiology." In Fazzaard , H . E .et al ., editor , THE HEART AND CARDIOVASCULAR SYSTWM , pages 1317 – 1341 . Raven PRESS , new York , 1986.

[5] R.E. Ideker and R.C. Barr, editors, Proceedings of the IEEE, Special Issue of ElectricaL Therapy of Cardiac Arrhythmias, volume 84, IEEE, 1996

[6] W. Müller, Windish, H. Tritthart, H.A. "Fluorescent Styryl Dyes applied as fast optical probes of cardiac action potential" Eur. Biophys. J. 1:103-111, 1986.

[7] H.P. Selker, "Coronary Care Unit Triage Decision Aids: How Do We Know When They Work?"Am. J. Med., 87:491-493, 1989.

[8] P. Kinias, H.A. Fozzard. "Rapid ECG Analysis and Arrhythmis Detection. " In L.D. Cady, editor, Computer Techniques in Cardiology, pages 97-122. Marcel Dekker Inc., New York/Basel, 1979.

[9] H.k. Wolf, P.J. MacInnis, S. Stock, R.K. Helppi, and P.M. Rautaharju. "Computer Analysis of Rest and Exercise Electrocardiograms." Comp. & Biom. Res., pages 329-346, 1972.

[10] W.D. Anderson, N.B. Wagner, K.L. Lee, R.D. White, Yuschak, et al. "Evaluation of a QRS Scoring System for Estimating Myocardial infarct size. VI: Identification of screening criteria for non-acute myocardial infarcts" Am. J. Cardiol., 61:729-733, 1988.

[11] Taccardi. "Distribution of Heart Potentials on the Thoracic Surface of Normal Human Subjects." Circ. Res., 1:341-351, 1963.

[12] Valtino X . Afonso , " ECG Beat Detection Using Filter Banks"IEEE vol . 46 , no 2 February 1999 pp . 192-202.

[13] Mohammed Abdel-Megeed Salem, Multiresolution Image Segmentation, Department of Computer Science, Humboldt-Universitaet zu Berlin, November 21, 2008, Berlin, Germany.

[14] Y.Y. Tang, J.Liu, L.H. Yang, H. Ma, "Wavelet Theory and its Application to Pattern Recognition", World Scientific Publishing Co. Pte. Ltd, 2000.

[15] Gerald Kaiser, "The Fast Haar Transform, Gateway to Wavelets", IEEE potentials, April/May, 1998.

[16] M. Misiti, Y.Misiti, G. Oppenheim, J. Poggi "Wavelet Toolbox User's Guide", 5th edition Mathworks. Inc.2007.

[17] Mohamed A. Tahoun, Mohamed Abdel-Megeed Salem, Khaled A. Nagaty, Taha I. El-Arief, "A Robust Content-Based Image Retrieval System Using Multiple Features Representations", IEEE International Conference on Networking, Sensing and Control (ICNS'05), March 10-22, 2005, Arizona, USA.

[18] M. Kania, M. Fereniec, R. Maniewski, Wavelet Denoising for Multi-lead High Resolution ECG Signals, MEASUREMENT SCIENCE REVIEW, Volume 7, Section 2, No. 4, 2007.

[19] Daubechies I: Ten lectures on wavelets, SIAM, Philadelphia, 1992.

[20] Abdel-Rahman Al-Qawasmi, Khaled Daqrouq, ECG Signal Enhancement Using Wavelet Transform, WSEAS TRANSACTIONS on BIOLOGY and BIOMEDICINE, issue 2, Volume 7, April 2010.

[21] Ramesh D.Mali, Mahesh S. Khadtare, U.L Bombale, Removal of 50Hz PLI using Discrete Wavelet Transform for Quality Diagnosis of Biomedical ECG Signal, International Journal of Computer Applications (0975-8887) Volume 23-No.7, June 2011.

[22] Mohamed Abdel-Megeed Salem, "Application of the 3D Wavelet Transform on Lane Extraction on Traffic Monitoring Images", Wavelets and Applications, wave 2006, July 10-14, 2006, Lausanne, Switzerland

[23] Mohammed A-Megeed Salem "On the Selection of the Propoer Wavelet for Moving Object Detection", The 7th IEEE International Conference on Computer Engineering and Systems (ICCES'11), November 29 - 30, December 1, 2011, Cairo, Egypt.